Journal of Bioenergetics and Biomembranes, Vol. 25, No. 2, 1993

Discrete Steps in Dioxygen Activation—The Cytochrome Oxidase/O_2 Reaction

Gerald T. Babcock[1] and Constantine Varotsis[1]

Received November 18, 1992; accepted November 20, 1992

The kinetic constraints that are imposed on cytochrome oxidase in its dual function as the terminal oxidant in the respiratory process and as a redox-linked proton pump provide a unique opportunity to investigate the molecular details of biological O_2 activation. By using flow/flash techniques, it is possible to visualize individual steps in the O_2-binding and reduction process, and results from a number of spectroscopic investigations on the oxidation of reduced cytochrome oxidase by O_2 are now available. In this article, we use these results to synthesize a reaction mechanism for O_2 activation in the enzyme and to simulate time-concentration profiles for a number of intemediates that have been observed experimentally. Kinetic manifestation of the consequences of coupling exergonic electron transfer to endergonic proton translocation emerge from this analysis. Energetic efficiency in this process apparently requires that potentially toxic intermediate oxidation states of dioxygen accumulate to substantial concentration during the reduction reaction.

KEY WORDS: Time-resolved vibrational spectroscopy; redox-linked proton pump; oxygen activation.

INTRODUCTION

Owing to the unusual architecture and ligand-binding properties of the heme a_3-Cu_B active site in cytochrome oxidase, the reduction of O_2 at this catalytic center has been uniquely susceptible both to time-resolved spectroscopic investigation at room temperature (Gibson and Greenwood, 1963) and to study by low-temperature trapping methods (Chance *et al.*, 1975). Moreover, partial reversal of the forward reaction can be achieved to produce stabilized intermediate catalytic states by taking advantage of the energy-transducing properties of the enzyme (Wikström, 1989). From these approaches, the opportunity to construct a reasonably detailed mechanism for dioxygen reduction has arisen (see, for example, Oliveberg and Malmström, 1992; Babcock and Wikström, 1992; Varotsis *et al.*, 1993; Ogura *et al.*, 1991). A general and remarkable aspect of the mechanisms that have been proposed is the progressive slowing down of succeeding steps in the reaction. As opposed to other oxygen-metabolizing heme enzymes, the rate-determining step in dioxygen catalysis in cytochrome oxidase occurs late, not early, in the mechanism. The biological consequences of this behavior are significant, as it suggests that transitions in the protein associated with proton-pumping rate limit the dioxygen bond cleavage chemistry. Operationally, this behavior allows partially metabolized oxygen intermediates to accumulate to detectable levels, and direct detection of several discrete intermediates in O_2 activation has been achieved. These kinetic conditions, then, have provided the opportunity to investigate biological oxygen metabolism in cytochrome oxidase at a level that has not been approached in any other oxygen-metabolizing metalloenzyme.

In this article, the kinetic basis for the success of the Gibson–Greenwood flow/flash technique, which has been a major tool in providing high time-resolution insight into the oxidase/O_2 reaction, is reviewed briefly. We then summarize several key experimental

[1]The LASER Laboratory and Department of Chemistry, Michigan State University, East Lansing, Michigan 48824.

0145-479X/93/0100-0071$07.00/0

observations that have been made on the cytochrome oxidase/O_2 reaction. These are used in presenting a mechanistic interpretation of the data that are currently available, in assessing limitations in the flow/flash approach, and in considering further tests of the proposed reaction mechanism.

THE FLOW/FLASH TECHNIQUE: A UNIQUE CONSTELLATION OF RATE CONSTANTS

Stopped-flow kinetics techniques are inadequate for studying the spontaneous oxidation of cytochrome oxidase by O_2, as the reaction is complete within the dead time of conventional stopper-flow mixers. The flow/flash technique overcomes this limitation by using CO to stabilize the reduced enzyme in the presence of O_2 for times sufficient to allow mechanical mixing with oxygenated buffer (Gibson and Greenwood, 1963). A photolysis pulse is used to remove CO and initiate the reaction, once mixing is complete, and time-resolved spectroscopies can then be used to monitor the reaction time course.

Schematically, the reaction sequence can be represented as follows:

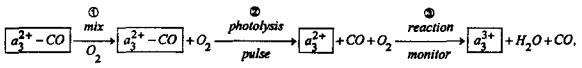

Scheme 1.

where a_3^{2+}–CO represents the CO complex of the reduced enzyme, a_3^{2+} represents the unliganded reduced enzyme, and a_3^{3+} represents the oxidized enzyme formed by reaction with O_2. If the flow/flash approach is to work effectively, several conditions must be met, as follows:

1. The thermal dissociation rate constant for CO(k_{off}) must be slow so that mechanical mixing with O_2 in Step 1 can occur without reaction.

2. The quantum yield for CO photolysis must be high to allow complete production of the unliganded, reactive reduced enzyme with single, short light pulses of moderate energy in Step 2.

3. The photodissociated CO must leave the a_3-Cu_B binuclear active site quickly following photolysis, and the heme pocket must relax rapidly, relative to the O_2-binding reaction.

4. The O_2/CO discrimination ratio, i.e., the ratio of the on-constant (k_{on}) for O_2 to that for CO, must be high, so that dioxygen chemistry, rather than trivial CO rebinding, occurs in the majority of the active sites during Step 3.

5. The oxygen on-constant, $k_{on}(O_2)$, must be large—ideally, it should be diffusion controlled—to prevent the binding reaction from becoming rate limiting and obscuring the subsequent electron and proton transfers and O–O bond-cleavage chemistry that are the phenomena of primary interest.

Although these are stringent conditions, all five are met in using flow/flash to study cytochrome oxidase. As with other heme carbonyls, the a_3^{2+}–CO complex photodissociates with a quantum yield that approaches unity and satisfies Requirement 2. The compilation of rate constants for cytochrome oxidase and several other heme systems in Table I shows that the oxidase–CO–O_2 system uniquely meets Points 1, 4, and 5. Thus, the k_{off}(CO) value for cytochrome oxidase, $0.023\,s^{-1}$, indicates that the carbon monoxy enzyme has a half-life of 30 s in the presence of O_2, which meets Point 1, above. The discrimination ratio $k_{on}(O_2)/k_{on}(CO)$, for oxidase is 1.4×10^3, compared to typical values of 5–30 for the other systems in Table I. The molecular basis for the high discrimination ratio in oxidase is not understood at present, but it does, nonetheless, satisfy Requirement 4 above. Finally, the absolute value for $k_{on}(O_2)$, $10^8\,M^{-1}\,s^{-1}$, is close to diffusion control, as required by Point 5.

Requirement 3 specifies that, following photolysis, the departing CO not interfere with incoming O_2 and that the enzyme be at thermal equilibrium as O_2 binds. There has been concern over whether these conditions are met, but the available evidence suggests that the oxidase reaction satisfies them. Gibson and his co-workers have examined these issues on several occasions and have found, for example, that the enzyme at 1 μs following CO photodissociation has optical absorption characteristics indistinguishable from those of the relaxed, reduced enzyme (Ludwig and Gibson, 1981). More recently, Blackmore *et al.* (1991) studied NO binding following CO photolysis and found rates for this process that are proportional to NO concentration up to pseudo-first order values of more than $10^5\,s^{-1}$, from which they conclude that there is no evidence of rate limitation exerted by departing CO in the flow/flash experiment, at least when NO is the incoming ligand. Findsen *et al.* (1987) examined the relaxation time course for the a_3^{2+} Fe-his vibration following CO photolysis. They found that its return to its thermal frequency was relatively slow, but, nonetheless, complete within microseconds of the photodissociating laser pulse, which is sufficient for flow/flash purposes. Woodruff and his co-workers have studied CO photolysis in detail, as summarized

Table I. Rate and Equilibrium parameters for the Reaction of CO and O_2 with Several Heme-Containing Systems[a]

	k_{on}(CO) ($M^{-1}s^{-1}$)	k_{off}(CO) (s^{-1})	K_{eq}(CO) (M^{-1})	$k_{on}(O_2)$ ($M^{-1}s^{-1}$)	D[b]
Cytochrome oxidase	7×10^4	0.023	3×10^6	1×10^8	1400
P-450$_{cam}$ + cam	3.7×10^4	0.14	2.6×10^5	7.7×10^5	20
Cytochrome *c* peroxidase	2×10^3	0.0092	2.2×10^5	4.5×10^4	23
Model heme	8.2×10^6	0.025	3.3×10^8	3.5×10^7	4
R-state hemoglobin α chains	6.5×10^6	0.01	6.5×10^8	5.9×10^7	9
Myoglobin (horse)	5×10^5	0.17	2.9×10^6	1.4×10^7	28
Leghemoglobin	1.3×10^7	0.016	7.9×10^8	1.2×10^8	9

[a]Data collected from Mims *et al.* (1983) and from Chang and Dolphin (1976). The model compound is protoheme mono-3-(1-imidazoyl) propylamide monomethyl ester in toluene (O_2 data) or benzene (CO data).
[b]'D' is defined as the ratio of $k_{on}(O_2)$ to k_{on}(CO).

elsewhere in this volume (Woodruff *et al.*, 1993). A key observation from this work is that CO, which binds transiently at Cu_B following its dissociation from a_3^{2+}, is released into solution with a half time of 1.5 μs. The α-band optical perturbation shows kinetics that parallel the appearance of CO in bulk solution. Taken together, experiments that have been designed to probe the time scale upon which the binuclear center relaxes to provide an unimpeded, thermalized binding site for dioxygen indicate that this occurs within 10 μs of CO photolysis. These processes are sufficiently fast that they do not appear to interfere with subsequent O_2 binding and reaction chemistry.

Despite this optimistic conclusion regarding the applicability of the flow/flash technique, two aspects of its implementation require further comment. First, in studying O_2 reduction by flow/flash, the fully reduced enzyme is usually used as the starting material. This state rarely occurs physiologically, and it is now clear that, in reducing O_2 from this initial redox configuration, only 50% efficiency in coupled proton translocation is achieved (Oliveberg *et al.*, 1991). The origin and implications of this "slippage" in proton translocation during the reaction of the fully reduced enzyme with O_2 has been discussed in detail elsewhere (Babcock and Wikström, 1992). Second, the oxidized form of the enzyme that is produced by flow flash has optical and magnetic characteristics that are different than those observed when fully reduced enzyme is mixed with O_2 in the absence of CO (Brunori *et al.*, 1979). Rousseau *et al.* (1992) have returned to this observation recently and have suggested that it may reflect secondary O_2 binding activity at Cu_B that occurs normally but is thwarted in the flow/flash experiment. The observation is intriguing and its significance is only just now beginning to be considered.

O_2 REDUCTION: BALANCING ENERGY TRANSDUCTION REQUIREMENTS AGAINST POTENTIAL OXYGEN TOXICITY

The original Gibson/Greenwood results with the flow/flash technique showed that the reduction of O_2 by cytochrome oxidase is biphasic (Gibson and Greenwood, 1963, 1967). The faster phase occurs in the first 100 μs, the slower phase has a characteristic time of about 800 μs, and both are accompanied by optical absorption changes that indicate heme A oxidation. In terms of the metal oxidation state changes that occur during these phases, we can now describe this biphasic oxidation with the following scheme:

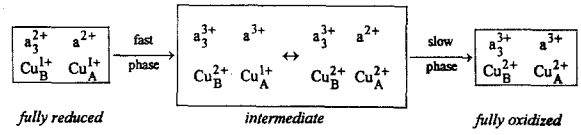

Scheme 2.

During the fast phase, the binuclear center and heme *a* are oxidized to form a three-electron oxidized intermediate state. In this intermediate, however, rapid electron transfer between Cu_A and heme *a* maintains a substantial fraction of heme *a* in its reduced state, as indicated by the double arrow in the center box in the above scheme. In the final, slow phase, the last electron is drained from the *a*/Cu_A pair.

The oxidant in the above reaction is, of course, O_2 and its reduction proceeds rapidly to the three-electron level in the intermediate state in the scheme above and then, more slowly, to the final, four-electron reduced, H_2O state. By necessity, this scheme requires that partially reduced oxygen intermediates are stabilized kinetically in the binuclear center. In view of the potential for toxic side reactions that could be

triggered by the presence of these highly oxidizing species, the benefits of a catalytic strategy that allowed the buildup of such intermediates was not apparent. The situation was clarified with Wikström's proton-pumping work that showed that the reduction of these free-energy rich, later intermediates in the reaction cycle is coupled to proton translocation in the energy-transducing reactions catalyzed by cytochrome oxidase (Wikström, 1981, 1989). Important conclusions and hypotheses follow from these observations (see also Babcock and Wikström, 1992):

1. Highly oxidizing intermediates in dioxygen reduction are stabilized for sufficient time to allow their subsequent reduction to be coupled to proton translocation.

2. If this is to occur efficiently, overall rate limitation in dioxygen activation is likely to be determined by events in the protein that are related to proton motion, rather than by the chemistry inherent to O—O bond cleavage.

3. With rate limitation transferred to proton translocation, *specific* intermediates in the oxygen reduction process may build up to detectable levels.

4. The binuclear center may be constructed primarily to facilitate the efficient coupling of proton translocation to oxygen reduction; i.e., structural features that are required for O_2 bond cleavage may not be inherent to the site, but only develop as the reaction proceeds. Such a strategy will allow exquisite control of the dioxygen chemistry.

O_2 REDUCTION: MOLECULAR INSIGHT INTO INDIVIDUAL STEPS IN THE PROCESS

The development of these ideas coincided with the continuing application of optical spectroscopy and the introduction of time-resolved Raman spectroscopy in studying the O_2/cytochrome-oxidase reaction. The Raman technique is especially useful, as it provides vibrational data and has the potential to establish the structure of bound, partially reduced oxygen intermediates. With these methods, it has been possible to add considerable structural and kinetic detail to the reduction time course in Scheme 2. Within each of the three chemical species in the scheme, several processes occur, and the two transitions in the reaction sequence also reflect more extensive chemistry. A more fundamental understanding of these processes is emerging. With Scheme 2 as a framework, the newer insights may be summarized as follows:

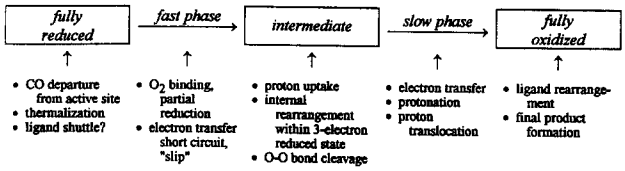

Scheme 3.

Several experimental observations have been important in developing the more detailed view of dioxygen reduction expressed above. In the following, these are discussed within the context of the processes indicated in Scheme 3.

The Fully Reduced Enzyme

The temporal evolution of the reduced enzyme following CO photolysis has been discussed above within the context of the flow/flash methodology. An important issue that was not considered there, however, is the proposed ligand shuttle model that Woodruff and co-workers have developed to account for observations that they and others have made during the relaxation following CO photolysis (Woodruff *et al.*, 1991, 1993; Rousseau *et al.*, 1992). Briefly, the Los Alamos group favors a model in which the photolyzed CO ligates Cu_B^{1+} and displaces a ligand, L, from this center. In the subsequent shuttle step, L migrates to the a_3^{2+} Fe and ligates the iron distally, displacing the proximal histidine. In an extension of the model, similar events—exogenous ligand binding at Cu_B^{1+}, L dissociation and migration to a_3^{2+}, and proximal histidine dissociation from the iron—are suggested to occur for small-molecule ligands, including O_2, that bind from solution. For O_2, there is support for transient O_2 binding at Cu_B *en route* to its a_3^{2+} destination (see below).

Some points require clarification and resolution within the ligand shuttle model, including the rate at which the Fe–L bond breaks, the identity of L, and the observation of the a_3^{2+} Fe-his vibration at short times following CO photolysis. The NO data from Blackmore *et al.* (1991) indicate that L dissociation from the a_3^{2+} iron does not rate limit NO binding to pseudo-first-order rates of $10^5\,s^{-1}$, which suggests that L dissociation is unlikely to affect O_2 binding to any significant extent. This observation, however, is difficult to reconcile with the idea that the CO on constant ($7 \times 10^4\,M^{-1}\,s^{-1}$) is rate limited by L dissociation. The identity of L remains to be established, although insight on this issue may be forthcoming from directed mutagenesis work now in progress (Hosler *et al.*, 1993). Finally, photolysis results for

both CO (Findsen *et al.*, 1987; Woodruff *et al.*, 1991) and for O_2 (Varotsis, C., Zhang, Y., and Babcock, G. T., in preparation) show that the a_3^{2+} ν(Fe-his) vibration is detected within nanoseconds following ligand dissociation. These observations can be reconciled with the occurrence of the ligand shuttle if the Fe–L bond is postulated to be photolabile (Woodruff *et al.*, 1991), and it will be interesting to see the results of work in progress on this issue (Woodruff *et al.*, 1993).

O_2 Binding and the Initial Electron-Transfer Steps

The O_2 binding reaction occurs during the fast phase in Scheme 3 and has intriguing properties. By inference from CO binding behavior (Lindsay *et al.*, 1975; Malatesta *et al.*, 1990), we expect that O_2 binding requires that both heme a_3 and Cu_B in the binuclear center be in their reduced states. Moreover, although Table I lists k_{on} (O_2) as a second-order rate constant, the heme a_3/oxygen-binding reaction saturates. Both Oliveberg and Malmström (1992) and Blackmore *et al.* (1991) interpreted this behavior to reflect transient binding of the incoming dioxygen at Cu_B in a true second-order reaction, followed by intramolecular, first-order transfer of O_2 to a_3. Blackmore *et al.* (1991) suggested that the second-order rate constant for Cu_B/O_2 association is $3.5 \times 10^8\,M^{-1}s^{-1}$; Oliveberg *et al.* (1989) have established the first-order reaction as proceeding at $\sim 9 \times 10^4\,s^{-1}$. These reactions are represented as the first two steps in Scheme 4, where the numbering system for specific intermediates introduced by Babcock and Wikström (1992) and extended by Varotsis *et al.* (1992) is preserved.

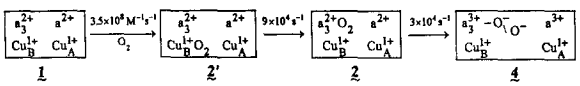

Scheme 4.

These reactions, at the rates indicated, are consistent with a growing body of experimental data. They rationalize the requirement for reduction of both a_3 and Cu_B prior to O_2 binding and the observation that O_2 binding to a_3 saturates. O_2 binding at a_3, but not at Cu_B, is expected to generate a substantial Soret absorbance charge, and Oliveberg *et al.* (1989) have observed that 40% of the total Soret absorbance change during dioxygen oxidation of the reduced enzyme occurs with an O_2 saturated rate of $9 \times 10^4\,s^{-1}$; the near IR changes that Oliveberg and Malmström (1992) later reported are likely to reflect the a_3^{2+}–O_2 association reaction as well. The $9 \times 10^4\,s^{-1}$ rate is also consistent with our time-resolved Raman data, which indicate little O_2 binding at 2 μs, but extensive a_3^{2+}–O_2 occupancy at 10 μs (Varotsis *et al.*, 1989). The frequency we and others observe for the $Fe_{a_3}^{2+}$–O_2 vibration, 572 cm^{-1} (Varotsis *et al.*, 1989, 1993; Han *et al.*, 1990a; Ogura *et al.*, 1990a), is well reproduced by our imidazole-heme *a*–O_2 model compound (Oertling *et al.*, 1990), which shows that there is little perturbation of the a_3–O_2 complex by distal pocket effects in the initial a_3^{2+}/oxygen adduct. Considering its arduous journey to its a_3 binding site, O_2 forms a relaxed, low-energy complex with the a_3 ferrous iron.

Both Raman and optical data support the decay of the a_3^{2+} oxy complex at a rate of $\sim 3 \times 10^4\,s^{-1}$, as shown in Scheme 4. Oliveberg *et al.* (1989) presented optical results showing that an additional 50% of the total change at 445 mm in the Soret of the reduced enzyme disappeared with this rate constant. The extent of this change is consistent with Raman data reported by both us (Varotsis and Babcock, 1990) and by Han *et al.* (1990b) in which substantial cytochrome *a* oxidation occurred at a rate comparable to the optical change. Babcock and Wikström (1992) have discussed this rapid cytochrome *a* oxidation reaction in detail recently and concluded that it represents the "slip" in the oxidase proton pump that reduces pumping efficiency to 50% when the fully reduced enzyme reacts with O_2. In the model they advanced, the formation of species 4 in Scheme 4 is preceded by transient Cu_B oxidation to form a peroxy intermediate they designated as 3. Reduction of 3, according to the $3 \times 10^4\,s^{-1}$ rate constant, is fast, and significant occupany of 3 during oxidation of the fully reduced enzyme is not observed.

Recent data reported by Blackmore *et al.* (1991) show that photolability in the oxidase reaction, which we had observed in our initial time-resolved Raman measurements on the reaction (Babcock *et al.*, 1984), persists substantially longer than predicted by the $3 \times 10^4\,s^{-1}$ rate constant. This observation has been reconciled recently with Scheme 4 by our demonstration that both oxy (2) *and* peroxy (4) intermediates in Scheme 4 are photolabile (Varotsis, C., Zhang, Y., and Babcock, G. T., in preparation). Taken together, the available results on O_2 binding and on the first electron-transfer reaction that are represented schematically as the fast phase in Scheme 3 can be accommodated by the molecular events shown in Scheme 4.

Internal Electron Rearrangement, Protonation, and O—O Bond Cleavage in the Three-Electron Reduced Enzyme

The fast phase of the reaction culminates in an intermediate species that contains three electrons in the oxygen-bound binuclear center, as shown in intermediate 4, above. Several important processes occur within the three-electron reduced enzyme, as initially emphasized by Chan and his co-workers (Blair *et al.*, 1985), and the rates and molecular details for some of these are now emerging. The electron input centers, heme *a* and Cu_A, equilibrate on the $1–2 \times 10^4 s^{-1}$ time scale, as a number of groups have now shown (Nilsson, 1992; Morgan *et al.*, 1989; Kobayashi *et al.*, 1989; Hill, 1993), by monitoring the equilibrium directly. In the dioxygen reaction, this redistribution reaction occurs with an apparent rate constant of $1 \times 10^4 s^{-1}$ (Oliveberg *et al.*, 1989) and is accompanied by an absorption increase in both the Soret and visible regions that had been perplexing in the initial flow/flash work. The redistribution reaction is shown as equilibrium 4 and 4′ in Scheme 5.

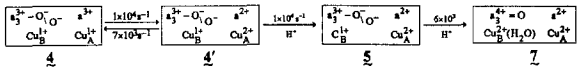

Scheme 5.

The peroxy structure in 4 and 4′ has not been detected directly by Raman or EPR spectroscopy; in the Raman experiments, we have been unable to detect oxygen-isotope sensitive vibrations immediately following the decay of the oxy species, 2. This changes fairly quickly, however, as a mode at $358 cm^{-1}$ ($342 cm^{-1}$ with $^{18}O_2$) appears with an onset of roughly $1 \times 10^4 s^{-1}$ in the Raman measurements (Ogura *et al.*, 1991; Varotsis *et al.*, 1993). This rate constant agrees well with the uptake of the first proton from solution (Oliveberg *et al.*, 1991), from which we infer that the protonated peroxy structure shown as intermediate 5 gives rise to the $358 cm^{-1}$, $\nu(Fe^{3+}_{a_3}-O^-)$, stetching vibration.

There appears to be a rigorous requirement for the input of the third electron into the binuclear center *before* the initial proton is taken up by the enzyme. If a flow/flash experiment is carried out with the half-reduced, mixed-valence enzyme, an oxy species identical to that formed by the fully reduced enzyme occurs transiently (Varotsis *et al.*, 1990; Han *et al.*, 1990d). Its lifetime is somewhat longer than that of 2, and it forms a stable peroxy species without proton uptake from solution (Oliveberg *et al.*, 1991). Despite the fact that the rapid input of the third electron in the oxidation of the fully reduced enzyme is not coupled to proton translocation, these observations, and particularly the electron-transfer-controlled proton uptake reaction in the fully reduced enzyme, are likely to reflect aspects of a regulatory mechanism for electron/proton coupling required in a redox-driven proton pump.

Cleavage of the O—O bond in 5 to produce the ferryl species 7 has not been time resolved accurately. In our time-resolved Raman work, however, we found that the $790 cm^{-1}$, oxygen-isotope sensitive mode that we assign as the $\nu(Fe^{IV}_{a_3}=O)$ vibration is not strongly enhanced until approximately 500 μs into the reaction. At this time, we no longer detect the $358 cm^{-1}$ vibration from 5. We could account for these results in a kinetic model in which the rate of decay of 5 into 7 was $\sim 6 \times 10^3 s^{-1}$ (Varotsis *et al.*, 1993). As Wikström (1989) has suggested that two protons are linked to the peroxy to ferryl transition, we associate a second protonation of 5 with its transformation to 7. Proton uptake from solution is not observed with this rate and, accordingly, we suggest that the second proton may already be associated with the fully reduced enzyme prior to reaction. Chan and his co-workers, as well, have stressed the likely activation of the O—O bond for cleavage by protonation (Blair *et al.*, 1985).

Even at the level of detail described in Scheme 5, the actual O—O bond cleavage reaction is not as well described as one would like. Additional intermediates that differ in protonation and valence are likely to occur in the 5 → 7 transition. At present, however, these species have escaped spectroscopic detection.

The Slow Phase of Reaction: Coupling Electron Transfer to Proton Translocation

Despite the high redox potential of the ferryl species (Wikström, 1989), our Raman data (Varotsis and Babcock, 1990), as well as those of Rousseau, Kitagawa, and this respective co-workers (Ogura *et al.*, 1990b; Han *et al.*, 1990c), indicate that this species accumulates to fairly high concentrations during the reoxidation reaction. Rate constants that have been reported for the transfer of the final electron electron are in the $10^3 s^{-1}$ range (Hill *et al.*, 1986), and our kinetic simulations (Varotsis *et al.*, 1993, and below) suggest that the slow phase in the oxidase reaction proceeds according to Scheme 6,

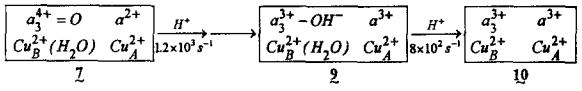

Scheme 6.

where, again, the numbering system for intermediate species has been preserved from that used by Babcock and Wikström (1992). The $\nu(Fe^{3+}-OH)$ vibration in the hydroxy intermediate, 9, has been detected by Raman by Han *et al.* (1990c) and by Varotsis *et al.* (1993).

Blair *et al.* (1985) have pointed out that cleavage of the O–O bond to form the ferryl proceeds with a relatively high activation energy; the input of the final electron is also highly activated (Oliveberg *et al.*, 1989). Moreover, in the fully reduced enzyme, reduction of the ferryl species is coupled to proton translocation, which indicates that, in this step, we have the opportunity to probe the full workings of the proton pump. Details remain murky, but the proton uptake measurements and pH dependence of the electron-transfer kinetics reported by the Göteborg group suggest that input of the fourth electron is necessarily preceded by protonation of a group with a pK_a of approximately 8.8 (Oliveberg *et al.*, 1989, 1991). The emergent theme is that electron motion is likely to be controlled by protonation events, under coupled conditions; rate limitation is transferred from oxygen chemistry to the proton transfer and conformational relaxation events associated with the proton pump. Interestingly, in the case of the transfer of the third electron to the binuclear center, electron transfer occurs prior to the protonation reaction (see above) and the pump is in a "slip" configuration. In the case of the final electron, protonation appears to rate limit electron transfer, and the pump is operational.

In view of recent directed mutagenesis results on terminal oxidases (Hosler *et al.*, 1993), it is possible to speculate on the identity of the $pK_a = 8.8$ residue that is involved with the final electron transfer. Helix VIII contains several conserved hydrophilic residues, including Thr-352, Thr-359, and Lys-362. Mutagenesis at any of these centers results in inactive enzyme. For Thr-352, the binuclear center is not assembled; in the case of mutations at the other two positions, a binuclear cluster is present, although with some structural modification. In a helical wheel representation of helix VIII, all three of these residues are on the same side of the structure but, in ascending residue number, lead away from the binuclear center to the inner side of the membrane. Such a structural arrangement is similar to the proton transfer pathways that have been suggested for H^+ delivery to the heme active site in $P450_{cam}$ (Raag *et al.*, 1991). In this enzyme, where x-ray structural data are available, hydrogen-bonded chains involving several side chains and solvent water molecules have been identified and implicated in controlling the rate and timing of proton delivery to the heme-bound dioxygen. Mutagenesis of one of the residues identified in this function, Thr-252, produced a $P450_{cam}$ enzyme in which electron transfer and substrate hydroxylation were uncoupled; either peroxide or water is produced instead. In considering the pK_a 8.8 residue identified kinetically in cytochrome oxidase and the apparent essential role of Lys-362 in preserving catalytic activity, it seems likely that this side chain plays a similar role in oxidase and is involved in gating the delivery of protons to the binuclear center during oxidase catalysis.

The Fully Oxidized Protein

The fully oxidized form of the enzyme is shown as the hydroxy species 9 in Scheme 6 above. This species, however, is unstable and decays through several intermediates, at least one of which is EPR detectable (Shaw *et al.*, 1979). The earlier data from Brunori *et al.* (1979), showing that the final form of the oxidized enzyme depends on whether flow/flash or multiple turnover conditions are used in the oxidation process, and the recent emphasis placed on this work by Rousseau *et al.* (1992) indicate that effort in the near future will be expended in understanding the relaxation of the initial oxidized state of the protein.

The Reaction Time Course

Schemes 4–6, above, provide a complete mechanism for the transition between fully reduced and fully oxidized cytochrome oxidase during its reoxidation by molecular oxygen in a flow/flash experiment. By using the rate constants in these schemes, we can simulate the time–concentration profiles for the major intermediates that we predict. Figure 1 shows the results of the simulation. The upper panel in Fig. 1 presents time–concentration curves for intermediates that occur in the first 400 μs of the reaction; the lower panel shows our calculated results over the first 2 ms. As we discussed above and elsewhere (Varotsis *et al.*, 1993), these time–concentration profiles are notable in showing that appreciable occupancy of intermediate species occurs at various times during the reaction. Undoubtedly, the maximum concentration calculated for some of the intermediates is an overestimate, particularly

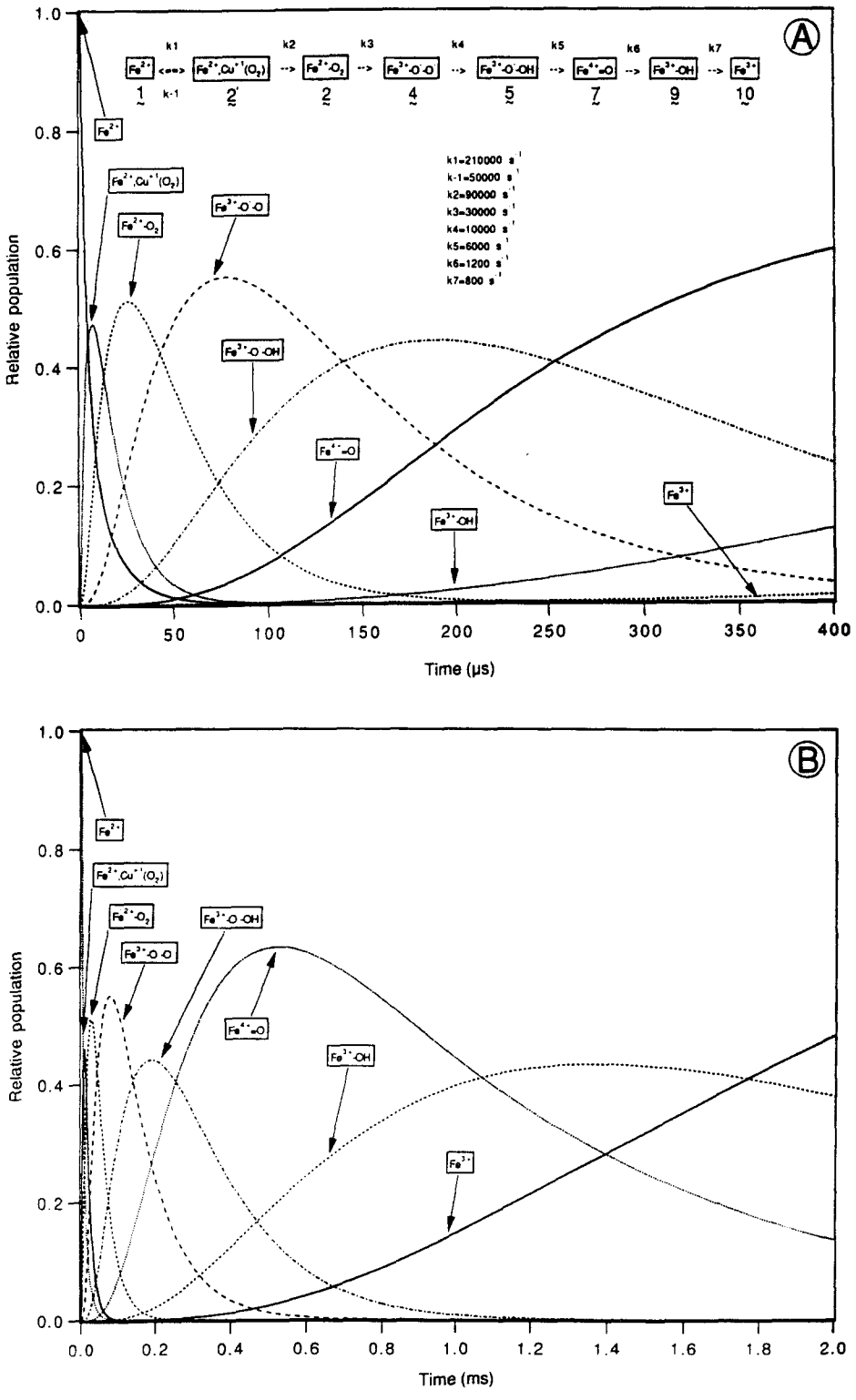

Fig. 1. Kinetic simulation of the reaction between reduced cytochrome oxidase and dioxygen. Panel A shows the first 400 μs of the simulation; Panel B shows the calculated time–concentration profiles over the first 2 ms. The kinetic scheme, rate constants, and numbering system for selected intermediates were taken from Schemes 4–6 in the text and are summarized in Panel A.

for those that occur later in the reaction, owing to protonation reactions and electronic rearrangements within the binuclear center that we have not yet been able to observe or take into account. Nonetheless, the progressive slowing down of the reaction, as it proceeds, which we interpret as reflecting a requirement of coupling the electron-transfer events associated with O_2 reduction to proton translocation, allows the concentration of several intermediates to increase to levels sufficient for their detection by time-resolved Raman spectroscopy (see Table II).

The individual reactions that comprise Schemes 4–6 are consistent with a significant body of flow/flash optical, proton uptake, and resonance Raman measurements on the reacting system, as discussed above. The last column in Table II shows the experimental delay times following reaction initiation over which the various intermediates are detectable by resonance Raman techniques. Comparison of these data with the simulations in Fig. 1 shows that the agreement is good; intermediates that rise to calculated concentrations of at least 40% of the initial enzyme concentration are detectable in the Raman experiments that have been carried out thus far. The exception to this is the initial peroxy intermediate 4, which appears to have escaped detection by us, by Kitagawa and his co-workers, and by Rousseau and his colleagues. Excitation profile effects may account for this discrepancy. Efforts are undoubtedly continuing to detect the vibrational signature of this important intermediate.

Table II. Oxygen-Isotope Sensitive Vibrations Detected in Flow/Flash, Time-Resolved Raman Measurements

Intermediate	Mode	$\bar{\nu}(cm^{-1}, {}^{16}O)$	$\bar{\nu}(cm^{-1}, {}^{18}O)$	Δt^a
2-Oxy	$\nu(Fe^{2+}-O_2)$	572	546	10–50 μs
5-Peroxy	$\nu(Fe^{3+}-\bar{O}OH)$	358	342	160–220 μs
7-Ferryl	$\nu(Fe^{4+}=O)$	790	755	300–800 μs
9-Hydroxy	$\nu(Fe^{3+}-OH)$	458 (450)[b]	434 (424)[b]	1–3 ms

[a] Time range following flash initiation of the O_2/cytochrome oxidase reaction over which the indicated vibration has been reported at room temperature.

[b] An 8–9 cm^{-1} difference exists in the frequencies reported for this mode by Varotsis *et al.* (1992) and by Han *et al.* (1990c).

CONCLUDING COMMENTS

The flow/flash approach has provided an incisive tool for a detailed dissection of the oxidation of reduced cytochrome oxidase. A variety of spectroscopic approaches have been implemented in conjunction with flash initiation of the reaction. These techniques provide complementary information that can be analyzed to construct a detailed mechanism for the ensuing reaction sequence, as shown above in Schemes 4–6 and in Fig. 1 (see also Varotsis *et al.*, 1992). The utility of the flow/flash technique is extended significantly by a striking aspect of the oxidase reaction that distinguishes it from other oxygen-metabolizing heme proteins, that is, the progressive slowing down of succeeding steps in the reaction, which allows several important intermediates to build up to detectable concentrations. We have argued above and elsewhere (Babcock *et al.*, 1992; Varotsis *et al.*, 1993, Babcock and Wikström, 1992) that this reflects the evolutionary choice to transfer rate limitation from dioxygen chemistry to protonation reactions and protein conformational shifts in order to drive proton translocation by the dioxygen redox chemistry.

There are, nonetheless, difficulties and ambiguities associated with the use of flow/flash with the reduced enzyme, a principal one being that the pumping efficiency is only half that occurs under more physiological conditions (Oliveberg *et al.*, 1991). This issue has been discussed to some extent above and in detail elsewhere (Babcock and Wikström, 1992). More generally, however, the reduced pumping efficiency reflects the fact that we start with a reduction state of the enzyme—all metal centers reduced—that is unlikely to occur under physiological conditions (Morgan and Wikström, 1991). As we analyze the flow/flash results more closely and attempt to integrate an expanding set of experimental results, it is also becoming apparent that we are likely to start from an unphysiological protonation state of the enzyme as well. We argued above, for example, that the first proton involved in binding substrate O_2 does so at a rate of $\sim 1 \times 10^4 s^{-1}$ from flow/flash proton uptake measurements carried out by the Göteborg group (Oliveberg *et al.*, 1991). With the fully reduced enzyme, however, it is possible, perhaps likely, that the site

from which the initial proton transfer occurs is preloaded and, thus, not detected in the bulk proton uptake measurements. Oliveberg *et al.* (1991) and Mitchell *et al.* (1992), in fact, have suggested that this may be the case. Thus, in using the flow/flash approach, it is useful to keep in mind its limitation, i.e., that it is a single turnover measurement in which the initial redox and protonation states are rarely achieved physiologically. Nonetheless, the pump functions in flow/flash, albeit at reduced efficiency, and the technique has given us an unprecedented opportunity to investigate the exquisite chemistry that takes place during dioxygen-bond cleavage and coupled proton translocation.

ACKNOWLEDGMENTS

The work described here was supported by NIH GM25480. We thank Mr. Yong Zhang for assistance in carrying out the computer simulations shown in Fig. 1.

REFERENCES

Babcock, G. T., and Wikström, M. (1992). *Nature (London)* **356,** 301–309.
Babcock, G. T., Jean, J. M., Johnston, L. N., Palmer, G., and Woodruff, W. H. (1984). *J. Am. Chem. Soc.* **106,** 8305–8306.
Babcock, G. T., Varotsis, C., and Zhang, Y. (1992). *Biochim. Biophys. Acta* **1101,** 192–194.
Blackmore, R. S., Greenwood, C., and Gibson, Q. H. (1991). *J. Biol. Chem.* **266,** 19245–19249.
Blair, D. F., Witt, S. N., and Chan, S. I. (1985). *J. Am. Chem. Soc.* **107,** 7389–7399.
Brunori, M., Colosimo, A., Rainoni, G., Wilson, M. T., and Antonini, E. (1979). *J. Biol. Chem.* **254,** 10769.
Chance, B., Saronio, C., and Leigh, J. S. (1975). *J. Biol. Chem.* **250,** 9226–9237.
Chang, C. K., and Dolphin, D. (1976). *Proc. Natl. Acad. Sci. USA* **73,** 3338–3342.
Findsen, E. W., Centeno, J., Babcock, G. T., and Ondrias, M. R. (1987). *J. Am. Chem. Soc.* **109,** 5367–5372.
Gibson, Q., and Greenwood, C. (1963). *Biochem. J.* **86,** 541–554.
Greenwood, C., and Gibson, Q. (1967). *J. Biol. Chem.* **242,** 1781–1787.
Han, S., Ching, Y.-C., and Rousseau, D. L. (1990a). *Proc. Natl. Acad. Sci. USA* **87,** 2491–2495.
Han, S., Ching, Y.-C., and Rousseau, D. L. (1990b). *Proc. Natl. Acad. Sci. USA* **87,** 8408–8412.
Han, S., Ching, Y.-C., and Rousseau, D. L. (1990c). *Nature (London)* **348,** 89–90.
Han, S., Ching, Y.-C., and Rousseau, D. L. (1990d). *Biochemistry* **29,** 1380–1384.
Hill, B. C. (1993), this volume.
Hill, B. C., Greenwood, C., and Nicholls, P. (1986). *Biochim. Biophys. Acta* **853,** 91–113.
Hosler, J. P., Ferguson-Miller, S., Calhoun, M. W., Thomas, J. W., Hill, J., Lemieux, L., Ma, J., Georgiou, C., Fetter, J., Shapleigh, J., Tecklenberg, M. M. J., Babcock, G. T., and Gennis, R. B. (1993), this volume.
Kobayashi, K., Une, H., and Hayashi, K. (1989). *J. Biol. Chem.* **264,** 7679–7980.
Lindsay, J. G., Owen, C. S., and Wilson, D. F. (1975). *Arch. Biochem. Biophys.* **169,** 492–505.
Ludwig, B., and Gibson, Q. H. (1981). *J. Biol. Chem.* **256,** 10092–10098.
Malatesta, F., Sarti, P., Antonini, G., Vallone, B., and Brunori, M. (1990). *Proc. Natl. Acad. Sci. USA* **87,** 7410–7413.
Mims, M. P., Porras, A. G., Olson, J. S., Noble, R. W., and Peterson, J. A. (1983). *J. Biol. Chem.* **258,** 14219–14232.
Mitchell, R., Mitchell, P., and Rich, P. R. (1992). *Biochim. Biophys. Acta* **1101,** 188–191.
Morgan, J. E., and Wikström, M. (1991). *Biochemistry* **30,** 948–958.
Morgan, J. E., Li, P. M., Jang, D.-E., El-Sayed, M. A., and Chan, S. I. (1989). *Biochemistry* **28,** 6975–6983.
Nilsson, T. (1992). *Proc. Natl. Acad. Sci. USA* **89,** 6497–6501.
Oertling, W. A., Kean, R. T., Wever, R., and Babcock, G. T. (1990). *Inorg. Chem.* **29,** 2633–2645.
Ogura, T., Yoshikawa, S., and Kitagawa, T. (1990a). *J. Am. Chem. Soc.* **112,** 5630–5631.
Ogura, T., Takahashi, S., Shinzawa-Itoh, K., Yoshikawa, S., and Kitagawa, T. (1990b). *J. Biol. Chem.* **265,** 14721–14723.
Ogura, T., Takahashi, S., Shinzawa-Itoh, K., Yoshikawa, S., and Kitagawa, T. (1991). *Bull. Chem. Soc. Jpn.* **64,** 2901–2907.
Oliveberg, M., and Malmström, B. G. (1992). *Biochemistry* **31,** 3560–3563.
Oliveberg, M., Brzezinski, P., and Malmstrom, B. G. (1989). *Biochim. Biophys. Acta* **977,** 322–328.
Oliveberg, M., Hallen, S., and Nilsson, T. (1991). *Biochemistry* **30,** 436–440.
Raag, R., Martinis, S. A., Sligar, S. G., and Poulos, T. L. (1991). *Biochemistry* **30,** 11420–11429.
Rousseau, D. L., Han, S., Song, S., and Ching, Y.-C. (1992). *J. Raman Spectrosc.*, in press.
Shaw, R. W., Hansen, R. E., and Beinert, H. (1979). *Biochim. Biophys. Acta* **548,** 386.
Varotsis, C., and Babcock, G. T. (1990). *Biochemistry* **29,** 7357–7362.
Varotsis, C., Woodruff, W. H., and Babcock, G. T. (1989). *J. Am. Chem. Soc.* **111,** 6439–6440.
Varotsis, C., Woodruff, W. H., and Babcock, G. T. (1990). *J. Am. Chem. Soc.* **112,** 1297.
Varotsis, C., Woodruff, W. H., and Babcock, G. T. (1993). *Proc. Natl. Acad. Sci. USA* **90,** 237–241.
Wikström, M. (1981). *Proc. Natl. Acad. Sci. USA* **78,** 4051–4053.
Wikström, M. (1989). *Nature* **338,** 776–778.
Woodruff, W. H., Einarsdottir, O., Dyer, R. B., Bagley, K. A., Palmer, G., Atherton, S. J., Goldbeck, R. A., Dawes, T. D., and Kliger, D. S. (1991). *Proc. Natl. Acad. Sci. USA* **88,** 2588–2592.
Woodruff, W. H., Dyer, R. B., and Einarsdottir, O. (1993), this volume.